Applied Mathematics and Computation 217 (2011) 8303–8310

Contents lists available at ScienceDirect

Applied Mathematics and Computation

journal homepage: www.elsevier.com/locate/amc

Analysis of spatial patterns in a vegetation model

Tao Guo [a,b], Qiulin Tan [b,*], Jijun Xiong [a]

[a] Science and Technology on Electronic Test and Measurement Laboratory, TaiYuan, Shanxi 030051, PR China
[b] Key Laboratory of Instrumentation Science and Dynamic Measurement (North University of China), Ministry of Education, TaiYuan 030051, PR China

ARTICLE INFO

Keywords:
Vegetation
Pattern
Rainfall
Self-organization

ABSTRACT

In this paper, a vegetation model with spatial diffusion is investigated. By linear analysis, we give the critical values of the wavenumber of the emerging patterns. Moreover, through a detailed analysis in two spatial dimensions, the pattern formation mechanisms of steady state patterns are obtained dependent on the quantity of rainfall. The mechanisms of pattern formation suggest that rainfall plays an important role in the formation of vegetation.

1. Introduction

In the past several decades, climatic changes and human activity have been leading to an unprecedented loss of habitats and species in ecosystems [8,15,25]. One of the most important problems is vegetation degradation. However, vegetation plays an very important role in the ecological environment. On one hand, it can prevent water loss and soil erosion, assimilate carbon dioxide and release oxygen from atmosphere to maintain the human beings and animals and contribute to the slowing of global warming, beautify the urban environment, protect us from sandstorms and so on. On the other hand, whether a change in vegetation pattern can indicate the loss or gain of resilience in real ecosystems is an good research question and needs to be better understood [19].

Vegetation pattern, have been extensively investigated by arid and semi-arid land ecologists [1,2,27,28]. The dominating driving forces in arid and semi-arid lands are lack of water and plant competition over water resources [29]. The view of vegetation patches as a pattern formation phenomenon involving symmetry breaking is supported by recent mathematical models that identify vegetation patterns with instabilities of uniform vegetation states [11,13,16,17]. As a result, this issue is usually treated in terms of determined reaction–diffusion models [11,13,16,17].

In particular, the vegetation equations modeled by Klausmeier [13] plays an important role in the study on vegetation patterns. The reason is that he firstly revealed the relationship between water and plant competition over water resources by a simple mathematical model, and discovered that striped patterns can grow lying along the contours of gentle slopes. From then on, many ecologists pay more attention to this model and the expanded versions of models which can also depict the interaction between water availability and plant growth. Sherratt studied the model by using linear stability and bifurcation analysis, and received the formulae of the wavelength and migration speed [20]. Moreover, nonlinear dynamics and pattern bifurcations in this model are also investigated [21]. They found that patterns exist for a wide range of rainfall levels and patterns with a variety of different wavelengths are stable.

However, Klausmeier's model only can explain the stripe pattern, and fails to account for spotted, hole and labyrinth pattern. Instead of investigating its model, we will give some analysis of the vegetation model which is presented by Meron et al. [18]. We want to check whether spotted, hole and labyrinth pattern can arise and see how rainfall has effect on the

* Corresponding author.
E-mail addresses: qiulintannuc2@163.com (Q. Tan), xiongjijun@nuc.edu.cn (J. Xiong).

0096-3003/$ - see front matter Crown Copyright © 2011 Published by Elsevier Inc. All rights reserved.
doi:10.1016/j.amc.2011.03.012

spatial patterns of the vegetation. The paper is organized according to the following orders: in Section 2, we present a vegetation model and interpret the biological meaning of these parameters. Mathematical analysis is given to obtain the critical wavenumber. In Section 3, we reveal the effect of rainfall on the spatial dynamics. Finally, some conclusions and discussion are given.

2. Model and bifurcation analysis

We firstly pay attention to the following model [18]:

$$\frac{\partial B}{\partial t} = \frac{GW}{1+SW}B - CB^2 - MB + D_B\nabla^2 B, \tag{1a}$$

$$\frac{\partial W}{\partial t} = P - I(1-RB)W - FW^2B + D_W\nabla^2(W - AB), \tag{1b}$$

where B and W represent the biomass density and the ground water density, respectively. The term $(GW/(1+SW))B$ describes plant growth at a constant rate, G/S, for saturated soil, and at a rate that grows linearly with W for dry soil. The term $-MB$ accounts for mortality and grazing, and the quadratic term $-CB^2$ represents saturation due to limited nutrients. P and term $-I(1-RN)W$ represent precipitation and a loss of source. Local up-take of water by plants is described by the term $-FW^2N$ [10]. The parameters R and A describe the positive feedback effects of water and biomass. $\nabla^2 = \partial^2/\partial x^2 + \partial^2/\partial y^2$ is the usual Laplacian operator in two-dimensional space. D_B and D_W are the diffusion coefficients. The meaning of the parameters can be found in Table 1.

In order to minimize the number of parameters involved in the model system it is extremely useful to write the system in non-dimensionalized form. Although there is no unique method of doing this, it is often a good idea to relate the variables to some key relevant parameters. Follow the method in Ref. [18], and take

$$b = \frac{C}{I}B, \quad w = \frac{F}{C}W, \quad \tilde{x} = \frac{I}{\sqrt{D_B}}x, \tag{2a}$$

$$\tilde{t} = It, \quad \gamma = \frac{C}{IF}G, \quad \sigma = \frac{C}{F}S, \quad \mu = \frac{M}{I}, \tag{2b}$$

$$p = \frac{I}{C}R, \quad \delta = \frac{D_W}{D_B}, \quad \beta = \frac{IF}{C^2}A, \tag{2c}$$

we arrive at the following equations containing dimensionless quantities:

$$\frac{\partial b}{\partial t} = \frac{\gamma w}{1+\sigma w}b - b^2 - \mu b + \nabla^2 b, \tag{3a}$$

$$\frac{\partial w}{\partial t} = p - (1-\rho b)w - w^2 b + \delta\nabla^2(w - \beta b). \tag{3b}$$

To study the turing instability, it is important to consider the local dynamics of the system obtained by setting the spatial derivatives equal to zero. The corresponding non-spatial model is

$$\frac{db}{dt} = \frac{\gamma w}{1+\sigma w}b - b^2 - \mu b = f(b,w), \tag{4a}$$

$$\frac{dw}{dt} = p - (1-\rho b)w - w^2 b = g(b,w). \tag{4b}$$

We are concerned the dynamics in the region $b \geqslant 0$ and $w \geqslant 0$. By considering the nullclines $f = 0,\ g = 0$, linear stability analysis reveals that model (4) has the following uniform stationary solutions:

Table 1
Parameter values used in the numerical simulation and nonlinear analysis are from the study of [10,18].

Symbol	Value	Unit	Comments
G	0.04	$mm^{-1}\ yr^{-1}$	Plant growth rate
S	0.01	mm^{-1}	Plant inhibition rate
C	4	$m^2/kg\ yr$	Saturation rate due to limited resource
M	0.8	yr^{-1}	Mortality and grazing rate
I	4	yr^{-1}	Loss rate of water due to evaporation and drainage
R	1.5	$mm^2\ kg^{-1}$	Increased rate of water due to plant
F	0.025	$m^4/kg^2\ yr$	Local up-take of water by plants
D_B	5×10^{-4}	$m^2\ yr^{-1}$	Diffusion coefficient of the plant
D_W	5×10^{-2}	$m^2\ yr^{-1}$	Diffusion coefficient of the water
β	3	–	–

(i) $E_1 = (0, p)$, which corresponds to bare soil;
(ii) $E^* = (b^*, w^*)$, which corresponds a uniform vegetation state, and

$$(\mu\sigma - \gamma)(w^*)^3 + C_2(w^*)^2 + C_1 w^* + p = 0, \tag{5a}$$

$$b^* = \frac{\gamma w^*}{1 + \sigma w^*} - \mu, \tag{5b}$$

where

$$C_1 = p\sigma - \rho\mu - 1, \tag{6a}$$

$$C_2 = \mu - \sigma - \rho\mu\sigma + \rho\gamma. \tag{6b}$$

From the biological point of view, we are interested in studying the stability behavior of the interior equilibrium point E^*, and the Jacobian matrix J is given by

$$J = \begin{pmatrix} \frac{\partial f}{\partial b} & \frac{\partial f}{\partial w} \\ \frac{\partial g}{\partial b} & \frac{\partial g}{\partial w} \end{pmatrix}\Big|_{(b^*, w^*)} = \begin{pmatrix} a_{11} & a_{12} \\ a_{21} & a_{22} \end{pmatrix},$$

where

$$a_{11} = \frac{\gamma w^*}{1 + \sigma w^*} - 2b^* - \mu, \quad a_{12} = \frac{\gamma b^*}{(1 + \sigma w^*)^2},$$

and

$$a_{21} = \rho w^* - (w^*)^2, \quad a_{22} = \rho b^* - 1 - 2b^* w^*.$$

Turing instability requires that the stable, homogeneous steady state is driven unstable by the interaction of the dynamics and diffusion of the species [22–24]. And the condition for the uniform steady state to be stable for the corresponding ordinary differential Eqs. (4a) and (4b) is given by

$$a_{11} + a_{22} < 0 \tag{7}$$

and

$$a_{11}a_{22} - a_{12}a_{21} > 0. \tag{8}$$

To linearize system (3) around E^* for small space- and time-dependent perturbations, we let

$$b(\vec{r}, t) = b^* + \bar{b}(r, t), \tag{9a}$$

$$w(\vec{r}, t) = w^* + \bar{w}(r, t). \tag{9b}$$

where $\bar{b}(r, t) \ll b^*$, $\bar{w}(r, t) \ll w^*$ and $r = (\mathbf{X}, \mathbf{Y})$ is spatial vector in two dimensions. We start by assuming solutions of the form

$$\begin{pmatrix} \bar{b}(r, t) \\ \bar{w}(r, t) \end{pmatrix} = \begin{pmatrix} \mu_1 \\ \mu_2 \end{pmatrix} e^{\lambda t} e^{i(k_{\mathbf{X}}\mathbf{X} + k_{\mathbf{Y}}\mathbf{Y})},$$

where λ is the growth rate of perturbation in time t, μ_1 and μ_2 represent the amplitudes, $k_{\mathbf{X}}$ or $k_{\mathbf{Y}}$ is the wave number of the solutions, and i represents imaginary number. The characteristic equation of the system (3) is

$$(H - \lambda I)\begin{pmatrix} \bar{b} \\ \bar{w} \end{pmatrix} = 0, \tag{10}$$

where

$$H = \begin{pmatrix} a_{11} - (k_{\mathbf{X}}^2 + k_{\mathbf{Y}}^2) & a_{12} \\ a_{21} + \delta\beta(k_{\mathbf{X}}^2 + k_{\mathbf{Y}}^2) & a_{22} - \delta(k_{\mathbf{X}}^2 + k_{\mathbf{Y}}^2) \end{pmatrix}. \tag{11}$$

We substitute $k^2 = k_{\mathbf{X}}^2 + k_{\mathbf{Y}}^2$ and derive the results for the two-dimensional case from one-dimensional formulation. As a result, we have characteristic polynomial of the original problem:

$$\lambda^2 - \mathrm{tr}_k\lambda + \Delta_k = 0, \tag{12}$$

where

$$\mathrm{tr}_k = a_{11} + a_{22} - (\delta + 1)k^2,$$
$$\Delta_k = a_{11}a_{22} - a_{12}a_{21} - (\delta a_{11} + a_{22} + \delta\beta a_{12})k^2 + \delta k^4. \tag{13}$$

The root of (12) can be obtained by the following form:

$$\lambda_k = \frac{1}{2}\left(\mathrm{tr}_k \pm \sqrt{\mathrm{tr}_k^2 - 4\Delta_k}\right). \tag{14}$$

It is easy to see that $\mathrm{tr}_k < a_{11} + a_{22}$. And thus we can conclude that for attractors and saddles a change of stability coincides with a change of the sign of Δ_k. By direct calculation, one can find that a change of sign in Δ_k occurs when k takes the critical values:

$$k_{1,2}^2 = \frac{(\delta a_{11} + a_{22} + \delta\beta a_{12}) \pm \sqrt{(\delta a_{11} + a_{22} + \delta\beta a_{12})^2 - 4\delta(a_{11}a_{22} - a_{12}a_{21})}}{2\delta}. \tag{15}$$

Furthermore, we have that

$$\Delta_k < 0 \Longleftrightarrow k_1 < k < k_2. \tag{16}$$

If both k_1 and k_2 exist and have positive values, they limit the range of instability for a local stable equilibrium. And this range is called as the Turing space. In order to see this space, we plot the dispersion relation corresponding to several values of one parameter while keeping the others fixed, see Fig. 1. Here, we set $\gamma = 1.6,\ \sigma = 1.6,\ \mu = 0.2,\ \rho = 1.5,\ \delta = 100,\ \beta = 3$ and vary p (The values of parameters can be found in Table 1.). It can be seen from this figure that when p is decreased, the available Turing modes $[\mathrm{Re}(\lambda) > 0]$ increase, and all available modes are enhanced further.

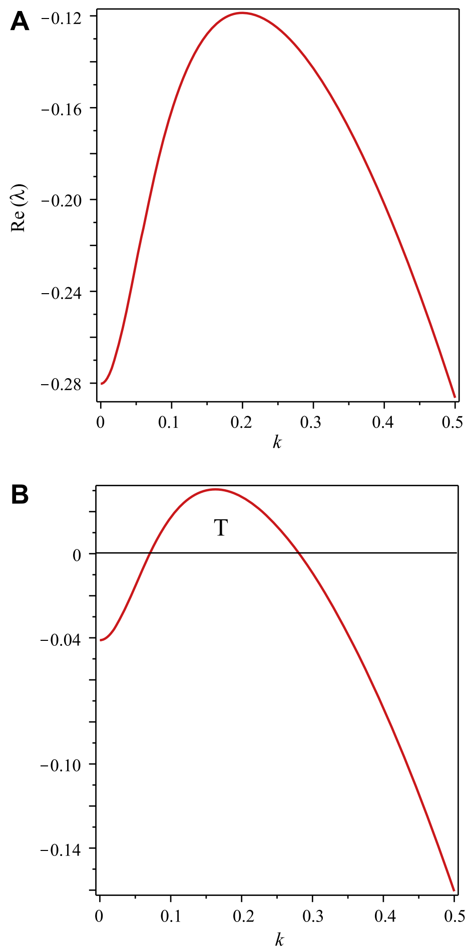

Fig. 1. These graphs illustrate the eigenvalues of the spatial model (3) at positive equilibrium point E^*. Parameter values are used: $\gamma = 1.6,\ \sigma = 1.6,\ \mu = 0.2,\ \rho = 1.5$. (A) $p = 0.6$; (B) $p = 0.4$.

3. Spatial patterns

In this section, we rely on numerical integration of the model of Eq. (3). We consider here spatiotemporal evolution of this system when the system lies within the regime of Turing domain. To solve differential equations by computers, one has to discretize the space and time of the problem. That is to say that transforming an infinite-dimensional to a finite-dimensional form. The two-dimensional space is solved in a discrete domain with $M \times N$ lattice sites. The spacing between each lattice point is defined by the lattice constant $\Delta h = 1$. And, the time evolution is solved by using the Euler method and $\Delta t = 0.001$.

The snapshots of the spatial patterns obtained at different time are shown in Fig. 2. It is evident that the initial random distribution ($t = 0$) is gradually replaced by black hole patterns ($t = 300$). The emergence of black hole patterns are formed by interaction of the vegetation and water, spread and eventually self-organize into a beautiful manifestation of pattern formation.

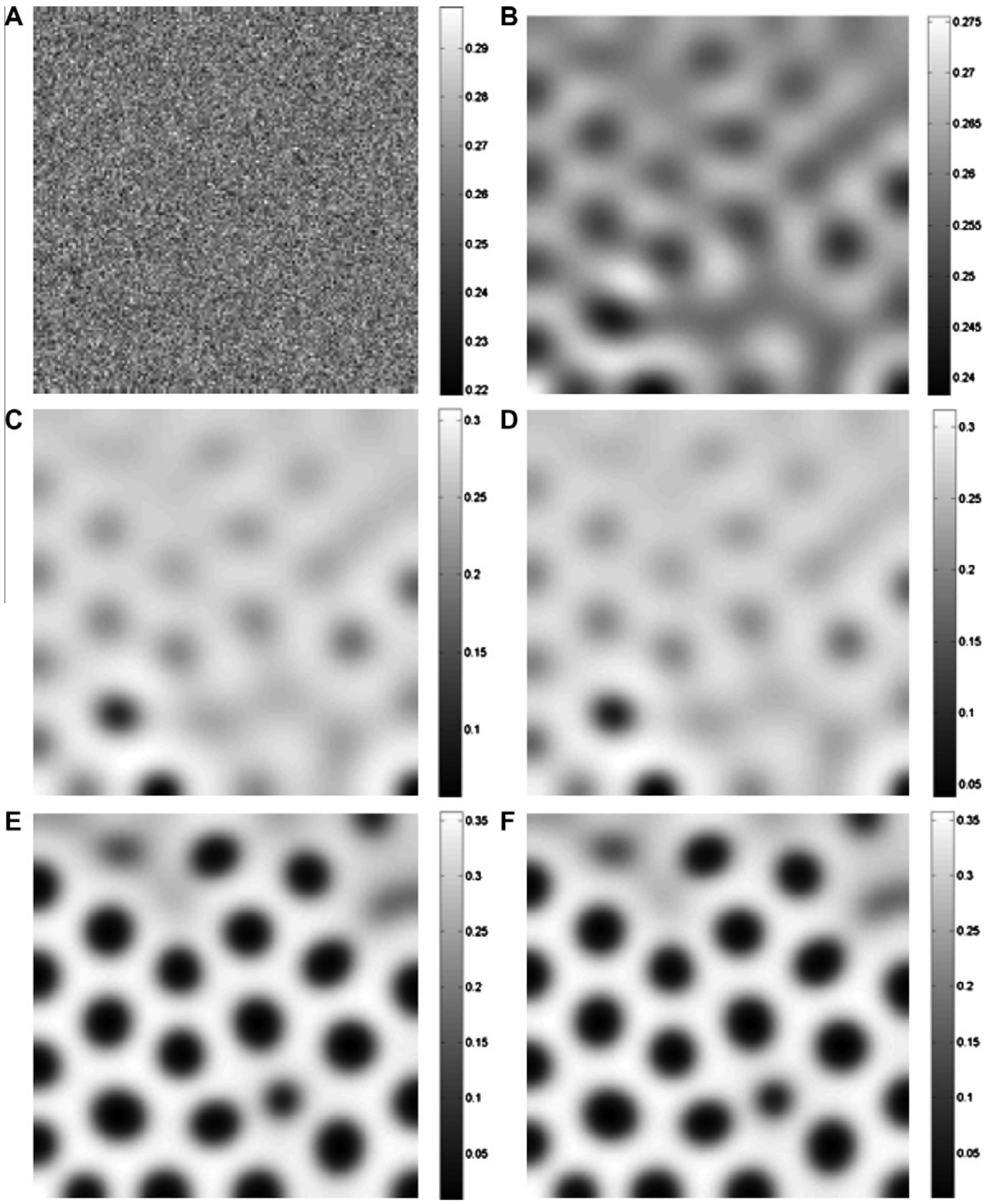

Fig. 2. Two-dimensional spatial patterns biomass generated by Eq. (3). Parameters values are used as: $\gamma = 1.6$, $\sigma = 1.6$, $\mu = 0.2$, $\rho = 1.5$, $\delta = 100$, $\beta = 3$ and $p = 0.6$. (A) $t = 0$; (B) $t = 50$; (C) $t = 80$; (D) $t = 100$; (E) $t = 180$; (F) $t = 300$.

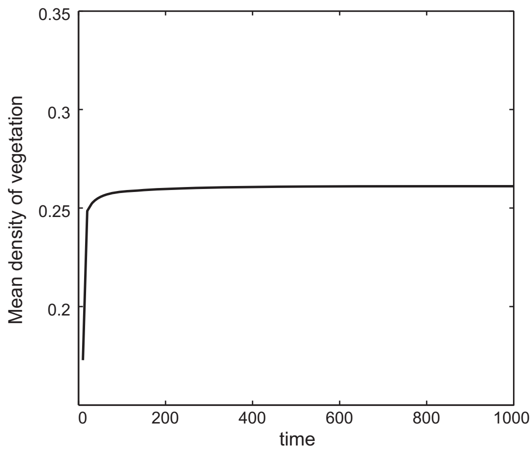

Fig. 3. Two-dimensional spatial patterns biomass generated by Eq. (3). Parameters values are used as: $\gamma = 1.6$, $\sigma = 1.6$, $\mu = 0.2$, $\rho = 1.5$, $\delta = 100$, $\beta = 3$, and $p = 0.4$.

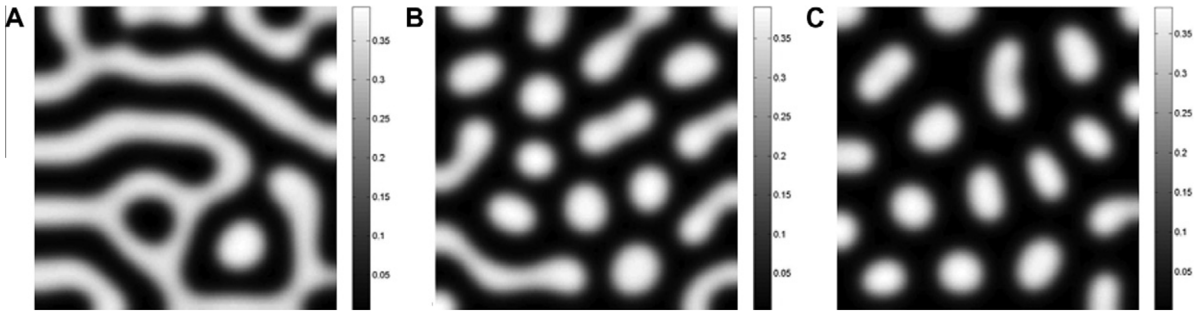

Fig. 4. Two-dimensional spatial patterns biomass generated by Eq. (3) at $t = 800$ with different values of p. Parameters values are used as: $\gamma = 1.6$, $\sigma = 1.6$, $\mu = 0.2$, $\delta = 100$, $\beta = 3$ and $\rho = 1.5$. (A) $p = 0.3$; (B) $p = 0.25$; (C) $p = 0.2$.

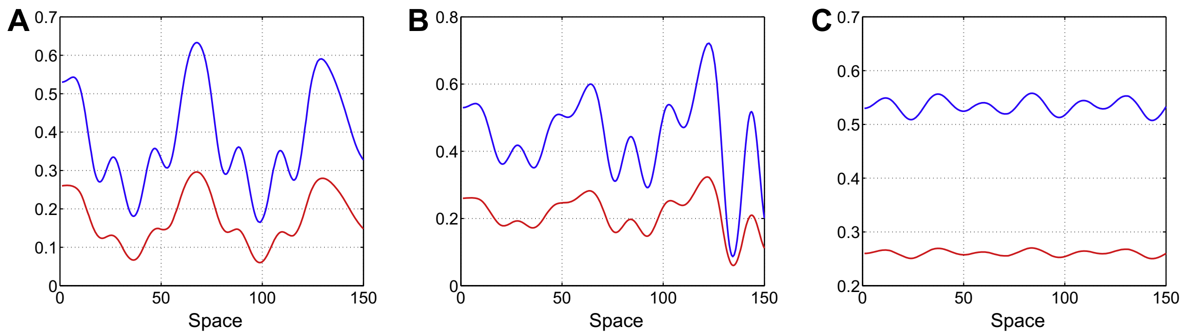

Fig. 5. Steady state profiles of vegetation computed in space using Eq. (17). Parameter values are used: $\gamma = 1.6$, $\sigma = 1.6$, $\mu = 0.2$, $\rho = 1.5$, $\delta = 100$ and $\beta = 3$. (A) $p = 0.3$; (B) $p = 0.25$; (C) $p = 0.2$.

A more precise temporal evolution of regular Turing pattern in the system can be visualized by means of the time series plot, as shown in Fig. 3. The temporal development of the spatially averaged values of the biomass density shows that in the first intervals of simulations these values change fast as the time increases. One can see that at $t \approx 50$, the density reaches a constant value and the mean value of the vegetation increases slower. At this time, the pattern formation has almost completely evolved. And the system has reached its steady state when $t > 100$.

However, the above results pertain to a fixed value of p, and thus it is of interest to investigate the impact of other values of p on pattern formation as well. In Fig. 4, we show the typical snapshots of the spatial grid obtained for different values of p after a long simulation time. As p decreases, labyrinth pattern, coexistence of spotted and striped pattern and spotted pattern only emerge successively.

To understand the evolution mechanism in space, we exploit the method of spatial dynamics, which was found to be an effective method exploring the multiplicity of steady state solutions [14,4,5,9,30,31]. To do so, we set $\partial b/\partial t = \partial w/\partial t = 0$ and rewrite (3) as a set of four first-order ordinary equations

$$\frac{db}{dx} = u, \tag{17a}$$

$$\frac{du}{dx} = -\frac{\gamma w}{1+\sigma w}b + b^2 + \mu b, \tag{17b}$$

$$\frac{dw}{dx} = v, \tag{17c}$$

$$\frac{dv}{dx} = \frac{-p + (1-\rho b)w + w^2 b + \beta\delta\left(-\frac{\gamma w}{1+\sigma w}b + b^2 + \mu b\right)}{\delta}, \tag{17d}$$

where space is now treated as a time-like variable. In Fig. 5, it shows that, for different p, the model always exhibits space oscillation. And for larger p, the amplitude of the oscillation is larger.

4. Discussion and conclusion

In this paper, we investigated a vegetation model in reaction–diffusion form. By performing both mathematical analysis and numerical simulations, we obtained rich spatial dynamics. Moreover, we found that, when p changes, hole, labyrinth, coexistence of spotted and striped and spotted pattern only emerge successively. In a word, rainfall plays an important in forming the vegetation patterns. In [18], they just do numerical simulations to account for vegetation patterns. However, in this paper, we give not only simulations results but also detailed analysis. Moreover, we provide the space evolution for different values of p.

Spatial self-organization is not imposed on any system but emerges from fine-scale interactions owing to internal causes. This process is key to understanding ecological stability and diversity [19]. Although more work is required, it seems that some vegetation models have many different kinds of regular spatiotemporal patterns. As a result, we can predict that the regular spatiotemporal patterns indicate that the ecosystems are more resilient to disturbance and resistant to global environmental change [19]. On the other hand, further studies are necessary to reveal which types of spatial patterns are the early-warning signals for the desert [12].

It should be noted that, in our model simulations, we have considered all the parameters as constants. However, vegetation and water are sometimes considered to be strongly influenced by seasonal factors such as weather and climatic conditions [6,7]. As a result, all the parameters can show temporal and spatial variations. In particular, some can be both stochastic and show significant seasonal variations [3,26], which will become a subject of future research.

Acknowledgments

We are grateful for the constructive suggestions of the anonymous referees on our original manuscript.

References

[1] M.R. Aguiar, O.E. Sala, Patch structure, dynamics and implications for the functioning of arid ecosystems, TREE 14 (1999) 273–277.
[2] J. Bascompte, R.V. Sole, Modeling Spatiotemporal Dynamics in Ecology, Springer-Verlag, Berlin, 1998.
[3] F. Borgogno, P. D'Odorico, F. Laio, L. Ridolfi, Mathematical models of vegetation pattern formation in ecohydrology, Rev. Geophys. 47 (2009) RG1005.
[4] J. Burke, E. Knobloch, Localized states in the generalized Swift–Hohenberg equation, Phys. Rev. E 73 (2006) 056211.
[5] J. Burke, E. Knobloch, Ladders: localized states in the Swift–Hohenberg equation, Phys. Lett. A 360 (2007) 681–688.
[6] C. Camporeale, L. Ridolfi, Noise-induced phenomena in riparian vegetation dynamics, Geophys. Res. Lett. 34 (2007) L18406.
[7] P. D'Odorico, F. Laio, A. Porporato, L. Ridolfi, Nicolas Barbier, noise-induced vegetation patterns in fire-prone savannas, J. Geophys. Res. 112 (2007) G02021.
[8] E. Gilad, J. von Hardenberg, A. Provenzale, M. Shachak, E. Meron, Ecosystem engineers: from pattern formation to habitat creation, Phys. Rev. Lett. 93 (9) (2004) 098105.
[9] D. Gomila, A.J. Scroggie, W.J. Firth, Bifurcation structure of dissipative solitons, Physica D 227 (2007) 70–77.
[10] D. Hillel, Environmental Soil Physics, Academic Press, San Diego, 1998.
[11] R. HilleRisLambers, M. Rietkerk, F. van den Bosch, H.H.T. Prins, H. de Kroon, Vegetation pattern formation in semi-arid grazing systems, Ecology 82 (2001) 50–61.
[12] S. Kefi, M. Rietkerk, C.L. Alados, Y. Pueyo, V.P. Papanastasis, A. ElAich, P.C. de Ruiter, Spatial vegetation patterns and imminent desertification in mediterranean arid ecosystems, Nature 449 (2007) 213–217.
[13] C.A. Klausmeier, Regular and irregular patterns in semiarid vegetation, Science 284 (1999) 1826–1828.
[14] E. Knobloch, Spatially localized structures in dissipative systems: open problems, Nonlinearity 21 (2008) T45–60.
[15] R. Leakey, R. Lewin, The Sixth Extinction, Doubleday, New York, 1996.
[16] R. Lefever, O. Lejeune, P. Couteron, in: P.K. Maini, H. Othmer (Eds.), Mathematical Models for Biological Pattern Formation IMA, vol. 121, Springer, New York, 2000, p. 83.
[17] O. Lejeune, M. Tlidi, A model for the explanation of vegetation stripes (tiger bush), J. Veg. Sci. 10 (1999) 201–208.
[18] E. Meron, E. Gilad, J. von Hardenberg, M. Shachak, Y. Zarmi, Vegetation patterns along a rainfall gradient, Chaos Solitons Fract. 19 (2004) 367–376.
[19] M. Rietkerk, J. van de Koppel, Regular pattern formation in real ecosystems, Trends Ecol. Evol. 23 (3) (2008) 169–175.
[20] J.A. Sherratt, An analysis of vegetation stripe formation in semiarid landscapes, J. Math. Biol. 51 (2005) 183–197.

[21] J.A. Sherratt, G.J. Lord, Nonlinear dynamics and patttern bifurcations in a model for vegetation stripes in semi-arid enviroments, Theor. Popul. Biol. 71 (2007) 1–11.
[22] G. Sun, Z. Jin, Q.-X. Liu, L. Li, Pattern formation in a spatial S-I model with non-linear incidence rates, J. Stat. Mech. (2007) P11011.
[23] G.-Q. Sun, Z. Jin, Q.-X. Liu, L. Li, Chaos induced by breakup of waves in a spatial epidemic model with nonlinear incidence rate, J. Stat. Mech. (2008) P08011.
[24] G.-Q. Sun, G. Zhang, Z. Jin, L. Li, Predator cannibalism can give rise to regular spatial pattern in a predator–prey system, Nonlinear Dyn. 58 (2009) 75–84.
[25] C.D. Thomas, A. Cameron, R.E. Green, M. Bakkenes, L.J. Beaumont, Y.C. Collingham, B.F.N. Erasmus, M.F. de Siqueira, A. Grainger, L. Hannah, L. Hughes, B. Huntley, A.S. van Jaarsveld, G.F. Midgley, L. Miles, M.A. Ortega-Huerta, A.T. Peterson, O.L. Phillips, S.E. Williams, Extinction risk from climate change, Nature (London) 427 (2004) 145–148.
[26] S. Thompson, G. Katul, S.M. McMahon, Role of biomass spread in vegetation pattern formation within arid ecosystems, Water Resour. Res. 44 (2008) W10421.
[27] D. Tilman, P. Kareiva, Spatial Ecology, Princeton University Press, Princeton, 1997.
[28] C. Valentin, J.M. dHerbes, J. Poesen, Water components of banded vegetation patterns, Catena 37 (1999) 1–24.
[29] J. von Hardenberg, E. Meron, M. Shachak, Y. Zarmi, Diversity of vegetation patterns and desertification, Phys. Rev. Lett. 87 (19) (2001) 198101.
[30] A. Yochelis, J. Burke, E. Knobloch, Reciprocal oscillons and nonmonotonic fronts in forced nonequilibrium systems, Phys. Rev. Lett. 97 (2006) 254510.
[31] A. Yochelis, Y. Tintut, L.L. Demer, A. Garfinkel, The formation of labyrinths, spots and stripe patterns in a biochemical approach to cardiovascular calcification, New J. Phys. 10 (2008) 055002.